Turkish Journal of Electrical Engineering & Computer Sciences

http://journals.tubitak.gov.tr/elektrik/

Research Article

Turk J Elec Eng & Comp Sci
(2018) 26: 2163 – 2177

doi:10.3906/elk-1804-116

Feature selection algorithm for no-reference image quality assessment using natural scene statistics

Imran Fareed NIZAMI[1,*], **Muhammad MAJID**[2], **Khawar KHURSHID**[1]
[1]School of Electrical Engineering and Computer Science, National University of Sciences and Technology, Pakistan
[2]Department of Computer Engineering, University of Engineering and Technology, Taxila, Pakistan

Received: 15.04.2018 • **Accepted/Published Online:** 16.07.2018 • **Final Version:** 28.09.2018

Abstract: Images play an essential part in our daily lives and the performance of various imaging applications is dependent on the user's quality of experience. No-reference image quality assessment (NR-IQA) has gained importance to assess the perceived quality, without using any prior information of the nondistorted version of the image. Different NR-IQA techniques that utilize natural scene statistics classify the distortion type based on groups of features and then these features are used for estimating the image quality score. However, every type of distortion has a different impact on certain sets of features. In this paper, a new feature selection algorithm is proposed for distortion identification based image verity and integration evaluation that selects distinct feature groups for each distortion type. The selection procedure is based on the contribution of each feature on the Spearman rank order correlation constant (SROCC) score. Only those feature groups are used in the prediction model that have majority features with SROCC score greater than mean SROCC score of all the features. The proposed feature selection algorithm for NR-IQA shows better performance in comparison to state-of-the-art NR-IQA techniques and other feature selection algorithms when evaluated on three commonly used databases.

Key words: No-reference image quality assessment, distortion identification based image verity and integration evaluation, feature selection, support vector regression, classification

1. Introduction

With the advancement in digital technology, multimedia content, especially images, have come into widespread use. Billions of images are shared over the Internet every day [1]. Images are affected by several types of distortion, due to imperfection in image acquisition systems and compression algorithms for storage and transmission. Therefore, evaluation methods that measure distortion in images have become significant. Image quality assessment (IQA) techniques have been broadly divided into objective and subjective quality measures [2]. Techniques that focus on finding features to assess the extent of distortion in an image without involving a human observer are known as objective methods, whereas image quality assessment performed by human observers is known as subjective evaluation, which is considered a benchmark for image quality evaluation. However, evaluation of each image by human observers is a laborious task that consumes a large amount of time. Therefore, a quantitative index that measures image quality is required. These techniques try to estimate the quality score of an image exclusive of any previous information about the nondistorted version of the image and this is known as no-reference image quality assessment (NR-IQA) [1, 3–5].

*Correspondence: 12phdinizami@seecs.edu.pk

Natural scene statistics (NSS) have been extensively utilized in NR-IQA techniques, as they work on the assumption that nondistorted images hold some particular statistical properties that are different from those of unnatural images [6, 7]. The effect of any type of distortion on an image makes it unnatural, resulting in changes in NSS properties. The divergence of the natural scene statistics of the image affected by distortion from the nondistorted image can be exploited to predict the perceived quality score of the image. NR-IQA is a difficult problem because of varying types of individual distortions and the diversity of content present in images. In the literature, several NR-IQA techniques based on NSS have been proposed [8–23]. Most NR-IQA techniques follow a two-step approach, i.e. determination of distortion type affecting the image and estimation of quality score using regression.

The blind image quality index (BIQI) uses a wavelet transform over three orientations and three scales and is parameterized by generalized Gaussian distribution (GGD) [24]. The shape parameter and standard deviation are used to compute the feature vector. A two-step approach using a support vector machine (SVM) classifier and regression is used in distortion identification based image verity and integration evaluation (DIIVINE) [2], in which a wavelet transform using steerable pyramids is computed for two scales and along six orientations to compute NSS features. A discrete cosine transform (DCT) is applied on 5×5 blocks of image to extract smoothness, texture, and edge information to assess the image quality using a Bayesian inference model in [25]. In [26], a codebook representation for no-reference image assessment (CORNIA) is proposed that used raw image patches to learn a codebook for NR-IQA. A blind/referenceless image spatial quality evaluator (BRISQUE) used the luminance coefficients of images, which are obtained using the empirical distribution of luminance, under the assumption that they represent NSS and can gauge the extent to which the image is affected by distortion [27]. In [1], joint normalization of the Gaussian Mixture (GM) map and Laplacian of Gaussian (LOG) is employed in an adaptive procedure for the calculation of IQA metrics based on non-Gaussianity (NG), local Gaussianity (LG), and exponential decay characteristics of NSS. A two-step framework using a curvelet transform is introduced in [3], where the feature set is based on the maxima of log histograms and the energy distribution of orientation and scale for the curvelet transform. An NR-IQA that extracts features in the spatial and spectral domain (SSEQ) is introduced in [4]. Spatial entropy is computed by dividing an image into blocks of 8×8 and the spectral entropies are computed on the DCT coefficients of the distorted image. In [18], NSS properties are improved by taking into account the fitting error, which occurs when irregularities in the distorted image are modeled using parameters for a distribution. In [28], an approach that measures the homogeneity in a block is proposed, where noise in the image is estimated by automatically locating homogeneous blocks and an adaptive averaging technique is applied that measures the noise in the image. Spatial contrast and structural distribution is considered in [29] for evaluating the quality score of images. The structural information variation metrics between the image gray-scale fluctuation map of the distorted and reference image is computed and are used as input to a pretrained support vector regression (SVR) model to predict the image quality. In [30], gradient histogram variation is used under a local transform to form global features for assessing the quality score of the image. In [8], a convolutional neural network is used for the extraction of features and SVR for mapping the extracted features to a quality score. An NR-IQA technique based on fragile watermarking and robust features is presented in [9]. Singular value decomposition is used for watermark extraction and the performance of IQA techniques is tested on various gray scale and color images.

All of the abovementioned NR-IQA techniques have used the same feature set for all distortion types to predict the quality of an image. However, each individual distortion type exhibits distinct characteristics, which

cannot be modeled using the same feature set. Therefore, distinct features for each individual distortion type should be selected. In this paper, a new feature selection algorithm is proposed, for the NSS based DIIVINE technique. DIIVINE is a two-step approach, i.e. distortion type soft classification followed by regression for IQA using the same features for each distortion type. The proposed technique differs from the DIIVINE algorithm in two aspects. Firstly, DIIVINE uses soft classification for prediction of the image quality score, whereas the proposed method uses hard classification for determination of the distortion type. Secondly, a feature selection module is added in the proposed method, which selects distinct features for each distortion type based on the mean value of the Spearman rank ordered correlation coefficient (SROCC) score. Recently, feature selection algorithms based on SROCC, linear correlation coefficient (LCC), Kendall correlation coefficient (KCC), and root mean squared error (RMSE) are proposed for NR-IQA [31], but the proposed algorithm is different from those algorithms in three aspects. First, the proposed feature selection is distortion specific, i.e. it selects different features for each distortion type, whereas the feature selection algorithms in [31] select the same features over all distortion types. Second, the proposed method performs feature selection based on five groups of statistical features, i.e. scale and orientation selective features, orientation selective statistics, correlation across scales, spatial correlation, and across orientation statistics. Only those feature groups are selected that have majority features with SROCC score greater than the mean SROCC score, which is computed over all the features, i.e. the bin size for feature selection is equal to the number of features in a particular feature group. In comparison, the algorithms in [31] perform feature selection on individual features, i.e. the bin size is equal to one feature. This has the disadvantage of losing inherent and detail information present in the whole feature group that can contribute to the overall performance and results in degradation of performance. Third, the selection of feature group seems logical since DIIVINE extracts features as groups, and so whether individual features in a feature group are utilized or discarded, all the features in a group have to be extracted, which does not contribute towards the reduction of execution time. The major contributions of the proposed method are as follows:

1. The proposed method helps in reducing the number of features used for NR-IQA, which makes the technique fast and efficient.

2. The feature selection improves the quality score prediction and shows better correlation with the mean observer score.

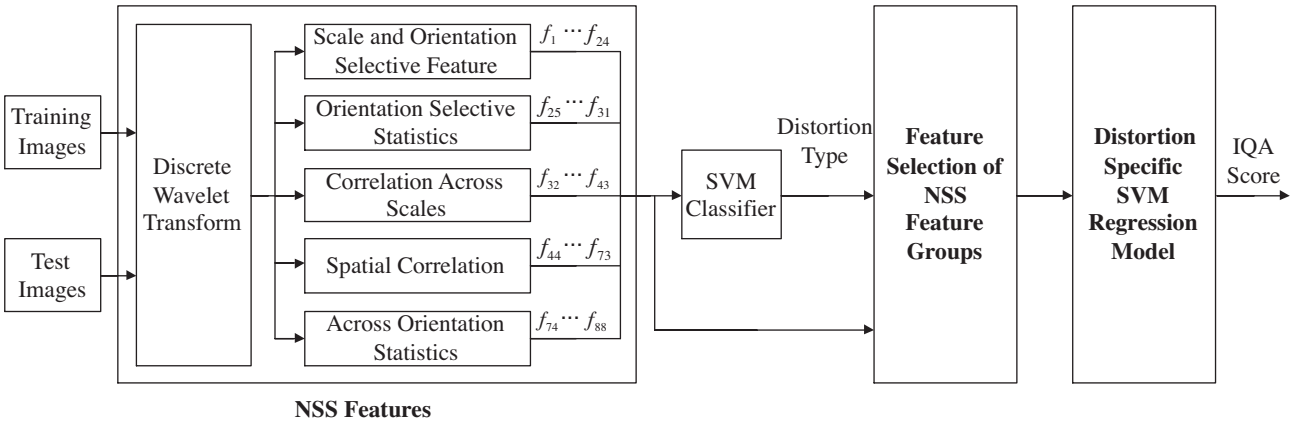

Figure 1. Block diagram of the proposed NR-IQA model using feature selection algorithm and regression.

The remainder of the paper is structured as follows. Section 2 describes the proposed methodology in detail. Experimental results and evaluations are reported in Section 3 followed by the conclusion in Section 4.

2. Proposed methodology

The block diagram of the proposed method for NR-IQA using feature selection algorithm is shown in Figure 1; it uses a three-step approach. Firstly, NSS based DIIVINE features are computed using a Gaussian scale mixture (GSM) and generalized Gaussian distribution (GGD). These features are used to determine the type of distortion affecting the image using an SVM classifier. In the second step, feature selection is performed for each distortion type based on mean SROCC score. Finally, a pretrained regression model, which is distortion specific, is utilized to predict the quality score of the image. Each step is explained in detail below.

2.1. Feature extraction

A loose wavelet transform that extracts features over two scales and six orientations (0^o, 30^o, 60^o, 90^o, 120^o, 150^o) is applied on images to obtain 12 subbands. The subbands of natural images have Gaussian distribution. A Gaussian scale mixture as given in [32] is used along with generalized Gaussian distribution to model the non-Gaussainity of distorted images. A GSM is calculated as

$$Y \equiv z \cdot U, \tag{1}$$

where Y is an N-dimensional random vector, U is a Gaussian random vector with zero mean and standard deviation σ_U, z is a mixing multiplier, and $\equiv$ represents equality in distribution. The vector Y models the marginal and joint statistics of the subbands. The density of Y is obtained by

$$p_Y(y) = \int \frac{1}{(2\pi)^{\frac{N}{2}}|z^2 C_U^{\frac{1}{2}}|} \exp\left(\frac{-Y^T C_U^{-1} Y}{z^2}\right) p_Z(z) dz, \tag{2}$$

where C_U is the covariance of the zero mean Gaussian random vector. The 12 subbands are further used to calculate five group of features, i.e. scale and orientation selective features containing $12 \times 2 = 24$ features that are obtained on 12 subbands to compute 2 parameters on each subband, i.e. variance and shape, orientation selective statistics consisting of 7 features where 6 features are obtained for shape parameters across 2 scales and at 6 orientations and the 7^{th} feature is obtained for the shape information from statistics across subbands, correlation across scales consists of 12 features that are obtained by computing the correlation between the high pass and low pass filter over each of the 12 subbands, spatial correlation has 30 features that are obtained by fitting the joint distribution of coefficients present at chess board distance to a third order polynomial, across orientation statistics containing ${}^6C_2 = 15$ features that are obtained on the coarsest level by computing the structural correlation. All these feature groups are concatenated to create a feature vector of length $24 + 7 + 12 + 30 + 15 = 88$. The details of the five groups of features are given below.

2.1.1. Scale and orientation selective features ($f_1 - f_{24}$)

This set of features is obtained by applying GGD to each of the 12 subbands. The choice of applying GGD is justified by the fact that in the absence of any distortion the scale and orientation selective features exhibit a Gaussian distribution, which is affected when an image is distorted. GGD is defined as

$$f_X(x; \mu, \sigma^2, \zeta) = a e^{-[bx-\mu]^\zeta}, \quad x \epsilon \Re \tag{3}$$

where μ and σ^2 represent the mean and variance of x respectively, ζ is the shape parameter ($\zeta = 1$ means Laplacian distribution, $\zeta = 2$ means Gaussian distribution), $a = \frac{b\zeta}{2\Gamma(\frac{1}{\zeta})}$, $b = \frac{1}{\sigma}(\frac{\Gamma(\frac{3}{\zeta})}{\Gamma(\frac{1}{\zeta})})^{\frac{1}{2}}$, and $\Gamma(\cdot)$ is calculated as

$$\Gamma(x) = \int_0^\infty t^{x-1}e^{-t}dt, \quad x > 0 \tag{4}$$

The wavelet subbands have zero mean and are only affected by variance and the shape parameter. Therefore, scale orientation features are calculated on the variance and shape parameter of the subbands separately.

2.1.2. Orientation selective statistics ($f_{25} - f_{31}$)

Digital images are inherently multiscale in nature and there exists a relationship between subbands at the same orientation but across different scales [2]. A GGD is well suited for the given objective and is used to increase the variation between the Gaussian distribution of each distortion type. GGD fit is used on all the coefficients of the subbands stacked together and only the shape parameter ζ is computed because standard deviation and mean do not contribute any information to the quality score.

2.1.3. Correlation across scales ($f_{32} - f_{43}$)

In the human visual system, the retinal ganglion cells possess the properties of filtering that can compute responses resembling the difference of Gaussian (DOG). This property can also help in enhancing high frequency features, which represent edges [33, 34]. Therefore, it is rational to assume the existence of a relationship between the high pass and band pass responses of an image [2]. These dependencies are captured by comparison of high pass band and low pass band correlations. A windowed structural correlation between the high pass and low pass components is calculated as

$$\rho = \frac{(2\sigma_{xy} + C_2)}{(\sigma_x^2 + \sigma_y^2 + C_2)}, \tag{5}$$

where σ_{xy} is the cross covariance between the band pass and high pass bands windowed regions, σ_x^2 and σ_y^2 denote the variances over the respective windowed regions, and C_2 is a constant, which stabilizes the output. The filters use a Gaussian window of 15×15 with $\sigma = 1.5$. The correlation across scales is calculated for each of the 12 subbands. The Gaussian window of different sizes has been used to extract edge and detail information from images for the purpose of IQA in state-of-the-art IQA techniques [35–39] with different Gaussian window sizes, i.e. 7×7, 8×8, 11×11 and 17×17 etc., which are all state-of-the-art. The window size of 17×17 is chosen because it gave the best results for DIIVINE [2].

2.1.4. Spatial correlation ($f_{44} - f_{73}$)

Natural images are extremely structured and variation in the spatial correlation structure of images is gradual [2]. When an image is affected by distortion, the natural structure is also disturbed regardless of the distortion type. The disturbance in the structure is recorded by using the joint empirical distribution $p_{XW}(x, w)$, which is approximated by using the chess board distance $\aleph_8^\tau(i, j)$ at spatial locations i and j and is given as

$$\rho(\tau) = \frac{e_{p_{XW}(x,w)}[(X - e_{p_X(x)}[X])^\tau - (W - e_{p_W(w)}[W])]}{\sigma_X \sigma_W}, \tag{6}$$

where $\rho(\cdot)$ estimates the correlation between X and W, τ is the distance, $e_{p_X(x)}[X]$ represents the expected value of X and its marginal distribution is given by $p_X(x), e_{pw(w)}[W]$ represents the expected value of W and its marginal distribution is given as $p_W(w)$, and $e_{p_{XW}}(x,w)[X]$ is the expected value of the joint distribution of x and w.

2.1.5. Across orientation statistics ($f_{74} - f_{88}$)

This group of features is obtained by utilizing six wavelet subbands at the coarsest level. The correlation across orientation is obtained by selecting two subbands out of six at a time, which leads to 15 combinations. Structural correlation as given in Eq. (6) is calculated by using a window of 15×15 on all the 15 combination of subband pairs.

Once feature extraction is performed, the next step is to classify the distortion type affecting the image. Any classifier can be used with the proposed methodology. In this work, an SVM classifier is selected because it has been shown to work well on high dimensionality data [2]. Let $(x_i, y_i)_{(1<i<M)}$ be the set of M training samples for the SVM classifier, where x_i is the i^{th} instance of a $M \times D$ feature vector, y_i is the i^{th} instance of a $M \times 1$ label vector such that $y_i \in \{+1, -1\}$, D is the feature set for one instance, and M is the total number of input samples. The aim of the SVM classifier is to obtain an optimum hyperplane so that all the samples that belong to one class should be on one side of the hyperplane and the samples that belong to the second class should be on the other side [40]. SVM is mathematically modeled as

$$f(x) = sgn(\sum_{i=1}^{M} \alpha_i y_i k(x_i, x) + b_1), \tag{7}$$

where $k(x_i, x)$ is the kernel function satisfying Mercer's theorem. Mercer's theorem states that there exists a mapping such that $k(x_i, x) = \Phi(x_i).\Phi(x)$, where, $\Phi(\cdot)$ is the mapping of x to the feature space, b_1 is the bias value, and α_i are the Lagrange multipliers, which maximize the function in Eq. (8).

$$W(\alpha) = \sum_{i=1}^{M} \alpha_i - \frac{1}{2} \sum_{i,j=1}^{M} \alpha_i \alpha_j y_i y_j \Phi(x_i) \Phi(x). \tag{8}$$

The input to the pretrained SVM classifier model is the DIIVINE features and the output is the distortion type. The LibSVM package is used to perform SVM classification, with a radial basis kernel function [41].

2.2. Feature selection

In this paper, the main aim is to select features based on SROCC, which are used to train and test the SVM regression model. Each distortion type affects images in different manner, i.e. Gaussian blur (GB) causes loss of edge information in the image, whereas images distorted with JPEG show distortion in the form of blockiness. As each distortion affects different characteristics of the image, it is not rational to use the same set of features for assessing the quality score of the image. In order to select features for each distortion type, the SROCC score is obtained against each individual feature. The SROCC is denoted by r_s and is calculated as

$$r_s = 1 - \frac{6 \Sigma d_i^2}{n(n^2 - 1)}, \tag{9}$$

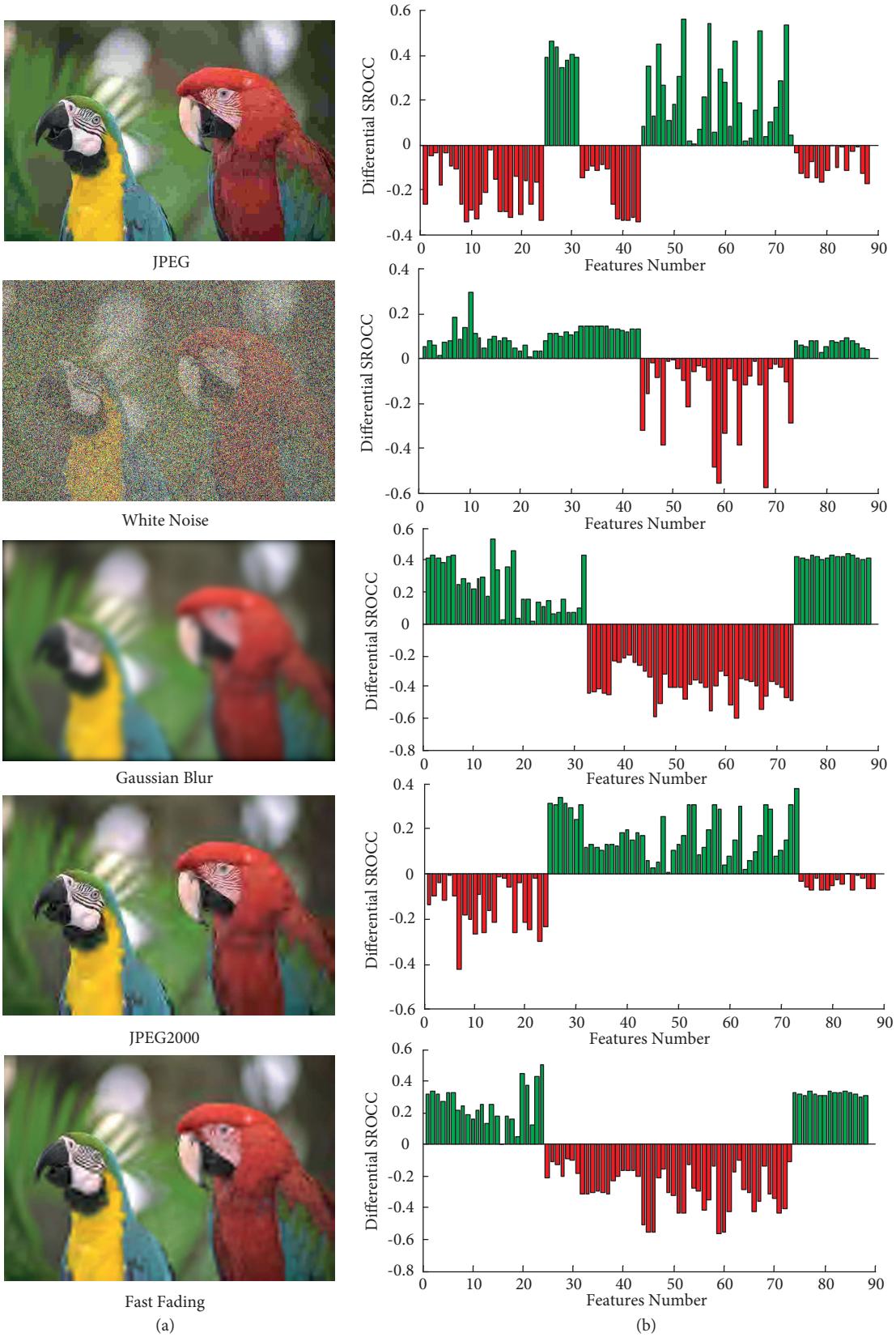

Figure 2. Differential SROCC of a single image for each distortion type. Column (a): distorted images, column (b): Differential SROCC.

where d_i represents the difference between paired ranks and n represents the total number of cases. SROCC score measures the coherence between the mean observer score and predicted quality score. A value close to 1 suggests superior performance. Hence, we select the feature group with the majority of the features having SROCC score greater than the mean SROCC score of all the features. Figure 2 shows the differential SROCC of each feature for different types of distortion. Differential SROCC is computed by taking the difference of SROCC score of each feature of the distorted image and the mean value of SROCC computed over training images. From Figure 2, it is clear that features have positive and negative values of differential SROCC for each type of

Algorithm 1: Feature Group Selection

Input :

1. DIIVINE features $F = f_1 - f_{88}$ of all images belonging to distortion type D.
2. Difference mean opinion score (DMOS) score of each image.
3. Length of each feature group: $L_{FG} = \{24, 7, 12, 30, 15\}$;

Output: F_G =feature group selected for distortion type D

for i=1 *to* 88 **do**
  Initialize to zero
  A = Array of thousand elements
  B = Array of eighty eight elements
  for *j=1 to 1000* **do**
    Randomly Select
    80% images for training
    20% images for testing
    Q = Predicted quality score
    A$(1, j)$ = SROCC(Q,DMOS) using Eq. (9)
  end
  B$(1, i)$ = median of A
end
μ = Mean value of B
for $k = 1$ *to 88* **do**
  if $B(1, k) > \mu$ **then**
    $F_0(1, k) = 1$;
  else
    $F_0(1, k) = 0$;
  end
end
$ind = 1$;
for l=1 *to* 5 **do**
  if $sum(F_0(1, ind : ind + L_{FG}(1, l) - 1) > L_{FG}(1, l)/2)$ **then**
    $F_G(1, l) = 1$;
  else
    $F_G(1, l) = 0$;
  end
  $ind = ind + L_{FG}(1, l)$;
end
return F_G;

distortion. Features having positive values of differential SROCC contribute to enhancing the performance of the NR-IQA technique, whereas features having negative values of differential SROCC contribute in degrading the performance of the NR-IQA technique. The proposed feature selection method is explained in Algorithm 1.

2.3. SVM regression

The feature groups are selected for each distortion type using the proposed Algorithm 1. The third and last step is to predict the quality score using distortion specific regression models. Each distortion specific regression model is trained using the feature groups having a majority of the features with SROCC score above mean SROCC value, i.e. each distortion type will have different features as input for the regression model. The SVM regression $\Psi(y)$ is given by

$$\Psi(y) = \beta\alpha(y) + c_1, \tag{10}$$

where y is denoted as the input vector, $\alpha(y)$ is the feature vector space, and β is the weight for the corresponding input. The transformation $\alpha(\cdot)$ relates the input vector to the feature space. If the training data are given by $\{y_i, x_i\}$, where y_i is the i^{th} input pattern, x_i is the corresponding target value and c_1 denotes the bias. The objective of SVM regression is to estimate $\Psi(y)$ such that the error between the target value and $\Psi(y)$ is minimized. All computations in SVM are performed using kernel function $k(m)$. The vector space does not have to be constructed explicitly when the inner product is computed using a kernel function. An L dimensional radial basis function with R centers is given as

$$k(y) = \Sigma_{n=1}^{R}\beta_i \frac{1}{(2\pi)^{\frac{|L|}{2}}\sigma_i^L} exp(-\frac{||y - c_i||}{2\sigma_i^2}) + b_2, \tag{11}$$

where c_i is the i^{th} Gaussian basis function center that has a standard deviation of σ_i, the weight of the i^{th} Gaussian basis function is represented as β_i, and b_2 is a constant.

3. Experimental results

3.1. Evaluation criteria and implementation details

The proposed methodology is based on machine learning techniques of classification and regression. Therefore, it requires training and calibration to predict image quality score. The dataset is split into nonoverlapping sets for training and testing. Images selected for training are not present in the test images, which negates the performance bias. The training set comprises 80% randomly selected images and the test set consists of the remaining 20% images. The training and testing are repeated 1000 times to predict the mean observer score and the median results are presented for performance evaluation. The support vector regression parameters c and γ are optimized for each NR-IQA technique using a grid search. Generally SROCC and linear correlation constant (LCC) are utilized to measure the performance of NR-IQA techniques. The linear correlation constant is given by

$$r_l = \frac{\sum_{i=1}^{n}(x_i - \bar{x})(y_i - \bar{y}))}{\sqrt{\sum_{i=1}^{n}(x_i - \bar{x})^2}\sqrt{\sum_{i=1}^{n}(y_i - \bar{y})}}, \tag{12}$$

where x_i and y_i are the MOS and predicted quality score of images respectively, the mean values of x_i and y_i are represented by $\bar{x}$ and $\bar{y}$ respectively, and n is the total number of samples.

3.2. Databases

In this work, the proposed methodology is tested on three of the most commonly used subjective IQA databases, i.e. LIVE [42], TID2008 [43], and CSIQ [44]. The LIVE database contains 29 nondistorted/reference images with five distortion types. There are 779 distorted images of varying degree in the LIVE database. The distorted images are categorized into five types of distortions namely GB, white noise (WN), JPEG2000 (JP2K) compression, JPEG compression, and fast fading (FF). The TID2008 database contains 25 nondistorted/reference images with 17 type of distortions, i.e. WN, additive noise in color components (ANC), spatially correlated noise (SCN), masked noise (MN), high frequency noise (HFN), impulse noise (IN), quantization noise (QN), GB, image denoising (ID), JPEG, JP2K, JPEG transmission errors (JTE), JPEG2000 transmission errors (JP2KTE), noneccentricity pattern noise (NEPN), local block-wise distortions of different intensity (LBDI), mean shift (MS), and contrast change (CC). The reference images are distorted at 4 different levels of each individual type of distortion. The image quality assessment is performed by observers from Ukraine, Finland, and Italy. Eight hundred experiments were performed, during which $256,000$ quality assessments were carried out. The evaluation on the TID2008 is done by more than 800 observers belonging to different social categories such as tutors, students, and researchers. The CSIQ database contains images with five distortion types. There are a total of 30 nondistorted/reference images and 866 distorted images. The images were shown to 35 observers on a LCD monitor with a resolution of 1920×1200. A total of 5000 individual image quality assessments were performed to calculate the mean observer score.

The output of experiments performed in the LIVE, CSIQ, and TID2008 databases is the image quality score of images that are computed by taking the average of individual perceptual quality scores for each image, as assessed by human observers. The LIVE and CSIQ databases provide the difference mean opinion score (DMOS), which represents the difference between the perceptual quality of pristine and distorted versions of the image and a lower value of DMOS suggests higher image quality. The TID2008 database provides MOS scores, which means a higher value of MOS suggests higher image quality. The range for DMOS values of the LIVE database is between 0 and 100, where 0 suggests the highest and 100 represents the worst image quality.

Table 1. Group of DIIVINE features selected by the proposed algorithm for each distortion type for LIVE database.

Feature Group	Distortion Type				
	JP2K	JPEG	WN	GB	FF
Scale and orientation selective subband coefficients ($f_1 - f_{24}$)	–	–	24	24	24
Orientation selective subband coefficients ($f_{25} - f_{31}$)	7	7	7	7	–
Correlation across scales ($f_{32} - f_{43}$)	12	–	12	–	–
Spatial correlation across subbands $f_{44} - f_{73}$)	30	30	–	–	–
Across orientation statistics ($f_{74} - f_{88}$)	–	–	15	15	15
Total Features Used	49	37	58	46	39
Percentage reduction in features as compared to DIIVINE	44.3%	57.9%	34.1%	47.72%	55.68%

The range for MOS of TID2008 is between 0 and 10, where 10 represents the highest and 0 represents the lowest image quality. The CSIQ database consists of DMOS scores ranging between 0 and 9, where a value close to 0 suggests higher and 9 suggests lower image quality.

3.3. Performance of the feature selection algorithm

The proposed method utilizes feature selection, which is explained in Algorithm 1. Only those feature groups are selected for a distortion type that have majority features with SROCC score greater than mean SROCC, for image quality evaluation. The groups of features selected for NR-IQA of each individual distortion type for LIVE databases the using proposed feature selection algorithm are summarized in Table 1. The mean SROCC score for the selection of the group of features for each distortion type is obtained by taking the average of individual feature SROCC scores over all three databases, i.e. the same group of features is used for performance evaluation over all the databases. It is evident that the maximum features selected are 58 for WN and minimum number of features selected are 37 for JPEG, which is 34.1% and 57.9% less than the total number of features used in the DIIVINE algorithm.

Table 2. Performance comparison of the proposed scheme for individual distortion types on the LIVE, TID2008, and CSIQ databases.

IQA Database	Distortion Type	BIQI [24]	BLINDS II [25]	BRISQUE [27]	DIIVINE [2]	CORNIA [26]	M3 [1]	CurveletQA [3]	SSEQ [4]	Improved NSS [18]	S [31]	SLKR [31]	Proposed
LIVE	JP2K	0.7849	0.9258	0.9175	0.8418	0.9271	0.9283	0.8914	0.8692	**0.9350**	0.7921	0.8210	0.9335
	JPEG	0.8801	0.9500	0.9655	0.8926	0.9437	**0.9659**	0.8370	0.8627	0.9310	0.8211	0.8421	**0.9659**
	WN	0.9157	0.9477	0.9789	0.9617	0.9608	0.9853	0.9700	0.9064	0.9860	0.8814	0.9205	**0.9887**
	GB	0.8367	0.9132	0.9479	0.8792	0.9553	0.9395	0.9340	0.9251	0.9560	0.8012	0.8414	**0.9681**
	FF	0.7023	0.8736	0.8854	0.8202	**0.9103**	0.9008	0.8153	0.8384	0.9080	0.7511	0.8011	0.9020
TID2008	WN	0.5368	0.6314	0.8603	0.7130	0.5941	**0.9338**	0.8722	0.8256	0.9150	0.6714	0.6823	0.9146
	GB	0.8878	0.9176	0.9059	0.8824	0.8941	0.9263	0.8475	0.8376	0.8960	0.8415	0.8531	**0.9557**
	ANC	0.1962	0.7282	0.5230	0.4235	0.2090	0.6250	0.5910	0.6470	0.7320	0.3014	0.3213	0.8873
	SCN	0.6992	0.8345	0.7790	0.7285	0.7185	0.7880	0.7790	0.8150	0.7932	0.6641	0.6823	**0.8745**
	MN	0.1935	0.3597	0.2990	0.3310	0.3610	0.3697	0.4960	0.5130	0.6125	0.2910	0.2935	**0.7797**
	HFN	0.6071	0.8523	0.8360	0.7754	0.7970	0.8546	**0.8650**	0.8250	0.8141	0.6921	0.7243	0.8494
	IN	0.0168	0.6681	0.8040	0.6792	0.5870	0.7766	0.6970	0.6910	0.7183	0.5514	0.6513	**0.7987**
	QN	0.6771	0.7899	0.6870	0.5935	0.7290	0.8161	0.8370	0.8010	0.7918	0.5161	0.5521	**0.8973**
	ID	0.7896	0.7568	0.5030	0.5563	0.7270	**0.8742**	0.7250	0.8760	0.8734	0.3814	0.5239	0.8735
	JPEG	0.8996	0.8853	0.9103	0.9033	0.9099	0.8812	0.8475	0.8075	0.9010	0.8714	0.8856	**0.9342**
	JP2K	0.8147	0.9118	0.9044	0.9103	0.9290	0.9068	0.8737	0.8722	0.8990	0.9001	0.9069	**0.9635**
	JPEGTE	0.5565	0.2572	0.2580	0.3042	0.5990	**0.7492**	0.4070	0.6380	0.7290	0.2214	0.2563	0.6591
	JP2KTE	0.5499	0.7590	0.7260	0.6775	0.6570	0.7072	0.7360	0.7260	0.8174	0.6012	0.6521	**0.8468**
	NEPN	0.1655	0.0842	0.2170	0.1781	0.1590	0.1999	0.1940	0.2242	0.3242	0.1004	0.1423	**0.4333**
	LBD	0.0992	0.3763	0.1990	0.1865	0.0190	0.3293	0.3190	0.3270	0.4161	0.1448	0.1624	**0.5904**
	MES	0.0097	0.1595	0.2190	0.1575	0.1870	0.2397	0.1290	0.2373	0.3732	0.0914	0.1120	**0.3977**
	CC	0.4263	0.0883	0.0890	0.1276	0.2680	0.2988	0.2260	0.3520	0.3609	0.0756	0.1023	**0.5325**
CSIQ	JP2K	0.7573	0.8870	0.8934	0.8692	0.8950	0.9406	0.7582	0.8120	**0.9450**	0.8012	0.8421	0.9430
	JPEG	0.8384	0.9115	0.9253	0.8843	0.8845	0.9328	0.7152	0.8283	0.9280	0.8015	0.8734	**0.9364**
	WN	0.6000	0.8863	0.9310	0.8131	0.7980	0.9172	0.9466	0.9123	0.8810	0.7914	0.8039	**0.9622**
	GB	0.8160	**0.9152**	0.9143	0.8756	0.9006	0.9070	0.7982	0.8318	0.8880	0.8610	0.8641	0.9108
Hit count		0	1	0	0	1	4	1	0	2	0	0	17

3.4. Performance comparison

The proposed methodology is compared with 11 state-of-the-art NR-IQA techniques, namely DIIVINE [2], BLINDS II [25], BRISQUE [27], BIQI [24], CORNIA [26], M3 [1], improved NSS [18], SA_IQA [29], S [31], and SLKR [31]. Table 2 shows the individual performance comparison of the proposed methodology for the LIVE, TID2008, and CSIQ databases, which validates the better performance of the proposed method. Table 2 also demonstrates that the proposed method performs better than state-of-the-art NR-IQA techniques and feature

selection algorithms over a majority of the distortion types. The proposed technique performs best for three out of five, 12 out of 17, and two out of four distortion types on the LIVE, TID2008, and CSIQ databases, respectively. The hit count and bold face values in Table 2 show the number of times a NR-IQA technique is ranked top. It can also be observed that the proposed method performs best with a hit count of 17, which is much higher than the best hit count of 4 for state-of-the-art NR-IQA techniques.

Table 3 shows the overall performance of the proposed method on individual IQA databases and the average performance on all three databases. It is evident that the performance of the proposed method is better

Table 3. Overall performance comparison of the proposed scheme in terms of median value of SROCC and LCC for the LIVE, TID2008, and CSIQ databases.

IQA Technique	LIVE		TID2008		CSIQ		Average	
	SROCC	LCC	SROCC	LCC	SROCC	LCC	SROCC	LCC
PSNR [45]	0.8890	0.8821	0.8789	0.8611	0.9292	0.8562	0.8978	0.8687
SSIM [46]	0.9486	0.9464	0.9032	0.9087	0.9362	0.9347	0.9345	0.9342
BIQI [24]	0.8084	0.8250	0.8438	0.8704	0.7598	0.8353	0.7995	0.8384
DIIVINE [2]	0.8816	0.8916	0.8930	0.9038	0.8697	0.9010	0.8800	0.8974
BLINDSII [25]	0.9302	0.9366	0.8982	0.9219	0.9003	0.9282	0.9131	0.9305
CORNIA [26]	0.9466	0.9487	0.8990	0.9347	0.8845	0.9241	0.9151	0.9373
BRISQUE [27]	0.9430	0.9468	0.9357	0.9391	0.9085	0.9356	0.9298	0.9414
M3 [1]	0.9511	0.9551	0.9369	0.9406	0.9243	0.9457	0.9390	0.9488
CurveletQA [3]	0.8875	0.9030	0.8602	0.8713	0.8045	0.7657	0.8534	0.8496
SSEQ [4]	0.8793	0.8899	0.8357	0.8577	0.8461	0.8707	0.8583	0.8762
Improved NSS [18]	0.9470	0.9500	0.9200	0.9260	0.9050	0.9250	0.9267	0.9361
SA_IQA [29]	**0.9658**	**0.9667**	0.8452	0.8660	0.9322	0.9392	0.9273	0.9347
S [31]	0.8094	0.8111	0.8211	0.8101	0.8137	0.8070	0.8147	0.8094
SLKR [31]	0.8452	0.8432	0.8319	0.8321	0.8458	0.8512	0.8410	0.8421
Proposed	0.9615	0.9623	**0.9420**	**0.9512**	**0.9381**	**0.9459**	**0.9455**	**0.9531**

Table 4. Comparison of proposed scheme in terms of number of features and execution time.

NR-IQA Technique	Average Number of features used	Execution Time (s)	Average SROCC	Average LCC
BIQI [24]	18	**0.076**	0.7995	0.8384
DIIVINE [2]	88	28.20	0.8800	0.8974
BLINDSII [25]	24	123.9	0.9131	0.9305
CORNIA [26]	20,000	3.246	0.9151	0.9373
BRISQUE [27]	36	0.176	0.9298	0.9414
M3 [1]	40	0.101	0.9390	0.9488
CurveletQA [3]	**12**	1.670	0.8875	0.8496
SSEQ [4]	**12**	2.680	0.8793	0.8762
Improved NSS [18]	56	0.332	0.9267	0.9361
SA_IQA [29]	81	1.570	0.9273	0.9347
S [31]	21	19.93	0.8147	0.8094
SLKR [31]	34	20.12	0.8410	0.8421
Proposed	58	21.09	**0.9455**	**0.9531**

than that of the state-of-the-art NR-IQA techniques. Furthermore, the proposed method performs equivalent to a full reference-IQA like PSNR and SSIM, which requires a nondistorted version of the image to estimate the perceived quality. The S [31] and SLKR [31] feature selection algorithms S and $SLKR$ [31] perform even worse than the DIIVINE NR-IQA technique because the S and $SLKR$ algorithms perform feature selection on individual features, which has the disadvantage of losing inherent and detail information present in the whole feature group that can contribute to the overall performance and results in degradation of performance.

Table 4 compares the average number of features used and the execution time in seconds for different NR-IQA techniques. The proposed method reduces the average number of DIIVNE features by 34.1% and results in better performance in terms of higher SROCC and LCC scores as compared to DIIVINE. The proposed method also reduces the execution time by more than 25.2% when compared to DIIVINE. The proposed method takes a longer time to compute the quality score than BIQI [24], CORNIA [26], BRISQUE [27], M3 [1], curveletQA [3], SSEQ [4], improved NSS [18], SA_IQA [29], S [31], and SLKR [31], but gives better performance in terms of average SROCC and LCC to predict the MOS.

4. Conclusion

Conventional NR-IQA techniques extract features to determine distortion type and then these features are used by the regression model to estimate the quality score of the image. An algorithm for feature selection is proposed in this paper, where different feature groups are selected for each distortion type. Only those feature groups are selected whose SROCC score is greater than the mean SROCC value of all extracted features using majority voting. The proposed method is evaluated over the LIVE, TID2008, and CSIQ databases. It is evident from the results that the predicted quality score using the proposed method shows high correlations with the subjective quality score represented by mean observer score. The proposed methodology shows better performance than the current NR-IQA techniques and other feature selection algorithms in terms of SROCC and LCC. The proposed method not only improves the estimation of quality score but also reduces the execution time and computational expense of the system as compared to the DIIVINE NR-IQA technique.

References

[1] Xue W, Mou X, Zhang L, Bovik AC, Feng X. Blind image quality assessment using joint statistics of gradient magnitude and laplacian features. IEEE T Image Process 2014; 23: 4850-4862.

[2] Moorthy AK, Bovik AC. Blind image quality assessment: From natural scene statistics to perceptual quality. IEEE T Image Process 2011; 20: 3350-3364.

[3] Liu L, Dong H, Huang H, Bovik AC. No-reference image quality assessment in curvelet domain. Signal Process-Image 2014; 29: 494-505.

[4] Liu L, Liu B, Huang H, Bovik AC. No-reference image quality assessment based on spatial and spectral entropies. Signal Process-Image 2014; 29: 856-863.

[5] Zhang M, Muramatsu C, Zhou X, Hara T, Fujita H. Blind image quality assessment using the joint statistics of generalized local binary pattern. IEEE Signal Proc Let 2015; 22: 207-210.

[6] Gao X, Gao F, Tao D, Li X. Universal blind image quality assessment metrics via natural scene statistics and multiple kernel learning. IEEE T Neur Net Lear 2013; 24: 2013-2026.

[7] Srivastava A, Lee AB, Simoncelli EP, Zhu SC. On advances in statistical modeling of natural images. J Math Imaging Vis 2003; 18: 17-33.

[8] Wu M, Chen L, Tian J. A hybrid learning-based framework for blind image quality assessment. Multidim Syst Sign P 2017; 29: 839-849.

[9] Bhattacharya A, Palit S. Blind quality assessment of image and video based on fragile watermarking and robust features. Multidim Syst Sign P 2017; 1-31.

[10] Nizami IF, Majid M, Afzal H, Khurshid K. Impact of feature selection algorithms on blind image quality assessment. Arab J Sci Eng 2018; 43: 4057-4070.

[11] Wu Q, Li H, Wang Z, Meng F, Luo B, Li W, Ngan KN. Blind image quality assessment based on rank-order regularized regression. IEEE T Multimedia 2017; 19: 2490-2504.

[12] Ma K, Liu W, Liu T, Wang Z, Tao D. dipiq: Blind image quality assessment by learning-to-rank discriminable image pairs. IEEE T Image Process 2017; 26: 3951-3964.

[13] Nizami IF, Majid M, Khurshid K. Efficient feature selection for blind image quality assessment based on natural scene statistics. In: IEEE 2017 International Bhurban Conference on Applied Sciences and Technology; 10–14 Jan 2017; Islamabad, Pakistan: IEEE. pp. 318-322.

[14] Wu Q, Li H, Ngan KN, Ma K. Blind image quality assessment using local consistency aware retriever and uncertainty aware evaluator, IEEE T Circ Syst Vid 2017; 1-12.

[15] Gu J, Meng G, Redi JA, Xiang S, Pan C. Blind image quality assessment via vector regression and object oriented pooling, IEEE T Multimedia 2018; 20: 1140-1153.

[16] Jenadeleh M, Moghaddam ME. Biqws: efficient wakeby modeling of natural scene statistics for blind image quality assessment. Multimed Tools Appl 2017; 76: 13859-13880.

[17] Li L, Yan Y, Lu Z, Wu J, Gu K, Wang S. No-reference quality assessment of deblurred images based on natural scene statistics. IEEE Access 2017; 5: 2163-2171.

[18] Zhang Y, Wu J, Xie X, Li L, Shi G. Blind image quality assessment with improved natural scene statistics model. Digit Signal Process 2016; 57: 56-65.

[19] Wang GJ, Wu ZY, Yun HJ, Cui M. No-reference image quality assessment based on nonsubsample shearlet transform and natural scene statistics. Optoelectronics Letters 2016; 12: 152-156.

[20] Xu J, Ye P, Li Q, Du H, Liu Y, Doermann D. Blind image quality assessment based on high order statistics aggregation. IEEE T Image Process 2016; 25: 4444-4457.

[21] Zhang Y, Moorthy AK, Chandler DM, Bovik AC. C-diivine: No-reference image quality assessment based on local magnitude and phase statistics of natural scenes. Signal Process-Image 2014; 29: 725-747.

[22] Liu L, Hua Y, Zhao Q, Huang H, Bovik AC. Blind image quality assessment by relative gradient statistics and adaboosting neural network. Signal Process-Image 2016; 40: 1-15.

[23] Wang T, Zhang L, Jia H, Li B, Shu H. Multiscale contrast similarity deviation: an effective and efficient index for perceptual image quality assessment. Signal Process-Image 2016; 45: 1-9.

[24] Moorthy AK, Bovik AC. A two-step framework for constructing blind image quality indices. IEEE Signal Proc Let 2010; 17: 513-516.

[25] Saad MA, Bovik AC, Charrier C. Blind image quality assessment: a natural scene statistics approach in the dct domain. IEEE T Image Process 2012; 21: 3339-3352.

[26] Ye P, Kumar J, Kang L, Doermann D. Unsupervised feature learning framework for no-reference image quality assessment. In: IEEE 2012 Conference on Computer Vision and Pattern Recognition; 16–21 June 2012. Providence, RI, USA: IEEE. pp. 1098-1105.

[27] Mittal A, Moorthy AK, Bovik AC. No-reference image quality assessment in the spatial domain, IEEE T Image Process 2012; 21: 4695-4708.

[28] Huang X, Chen L, Tian J, Zhang X, Fu X. Blind noisy image quality assessment using block homogeneity. Comput Electr Eng 2014; 40: 796-807.

[29] Yang X, Sun Q, Wang T. Image quality assessment via spatial structural analysis. Comput Electr Eng 2016; 1-17.

[30] Sun T, Ding S, Chen W, Xu X. No-reference image quality assessment based on gradient histogram response. Comput Electr Eng 2016; 54: 330-344.

[31] Nizami IF, Majid M, Khurshid K. New feature selection algorithms for no-reference image quality assessment. Appl Intell 2018; 1-20.

[32] Wainwright MJ, Simoncelli EP. Scale mixtures of gaussians and the statistics of natural images. Adv Neur In 2000; 855-861.

[33] Sekuler R, Watamaniuk SN, Blake R. Perception of Visual Motion, Steven's Handbook of Experimental Psychology. 3rd ed. New York, NY, USA: Wiley, 2002.

[34] Teo PC, Heeger DJ. Perceptual image distortion. In: IEEE 1994 International conference on Image Processing; 13–16 Nov 1994; Austin, TX, USA. IEEE. pp. 127-141.

[35] Zhang L, Zhang L, Bovik AC. A feature-enriched completely blind image quality evaluator. IEEE T Image Process 2015; 24: 2579-2591.

[36] Gu K, Zhou J, Qiao JF, Zhai G, Lin W, Bovik AC. No-reference quality assessment of screen content pictures. IEEE T Image Process 2017; 26: 4005-4018.

[37] Li Q, Lin W, Xu J, Fang Y. Blind image quality assessment using statistical structural and luminance features. IEEE T Multimedia 2016; 18: 2457-2469.

[38] Liu L, Liu B, Su CC, Huang H, Bovik AC. Binocular spatial activity and reverse saliency driven no-reference stereopair quality assessment. Signal Process-Image 2017; 58: 287-299.

[39] Fang Y, Yan J, Li L, Wu J, Lin W. No reference quality assessment for screen content images with both local and global feature representation. IEEE T Image Process 2018; 27: 1600-1610.

[40] Chapelle O, Haffner P, Vapnik VN. Support vector machines for histogram-based image classification. IEEE T Neural Networ 1999; 10: 1055-1064.

[41] Chang CC, Lin CJ. Libsvm: a library for support vector machines, ACM T Intel Syst Tec 2011; 2: 1-27.

[42] Sheikh HR, Sabir MF, Bovik AC. A statistical evaluation of recent full reference image quality assessment algorithms. IEEE T Image Process 2006; 15: 3440-3451.

[43] Ponomarenko N, Lukin V, Zelensky A, Egiazarian K, Carli M, Battisti F. Tid2008 - a database for evaluation of full-reference visual quality assessment metrics. Advances of Modern Radioelectronics 2009; 10: 30-45.

[44] Larson EC, Chandler DM. Most apparent distortion: full-reference image quality assessment and the role of strategy. J Electron Imaging 2010; 19: 011006-011006.

[45] Huynh-Thu Q, Ghanbari M. Scope of validity of psnr in image/video quality assessment. Electron Lett 2008; 44: 800-801.

[46] Wang Z, Bovik AC, Sheikh HR, Simoncelli EP. Image quality assessment: from error visibility to structural similarity. IEEE T Image Process 2004; 13: 600-612.